Brain Tumor Classification with Machine Learning for Computer Vision

Laura Madrid, Lucas Noritomi-Hartwig , Keshav Worathur

University of Toronto

Introduction

Brain tumours affect approximately 50,000 Canadians every year, according to the Brain Tumour Registry of Canada (BTRC) [5]. Manual diagnosis of brain tumours is time-intensive and requires specialized knowledge of the brain [4].

Research Questions

How can we build an efficient model to effectively classify glioma, meningioma, and pituitary tumors by improving current methods of detection and classification using brain MRI scans? Through what decision-making processes will the model classify brain tumors into the distinct categories?

Data Exploration & Augmentation

We used the **Figshare Brain Tumor Dataset** [3], which crucially includes patient-ID labels and the three tumor classes. This dataset contains 3,064 brain MRIs collected from 233 patients along the axial, coronal, and sagittal axes.

Tumor frequency from Figshare dataset.

Examples from Figshare dataset.
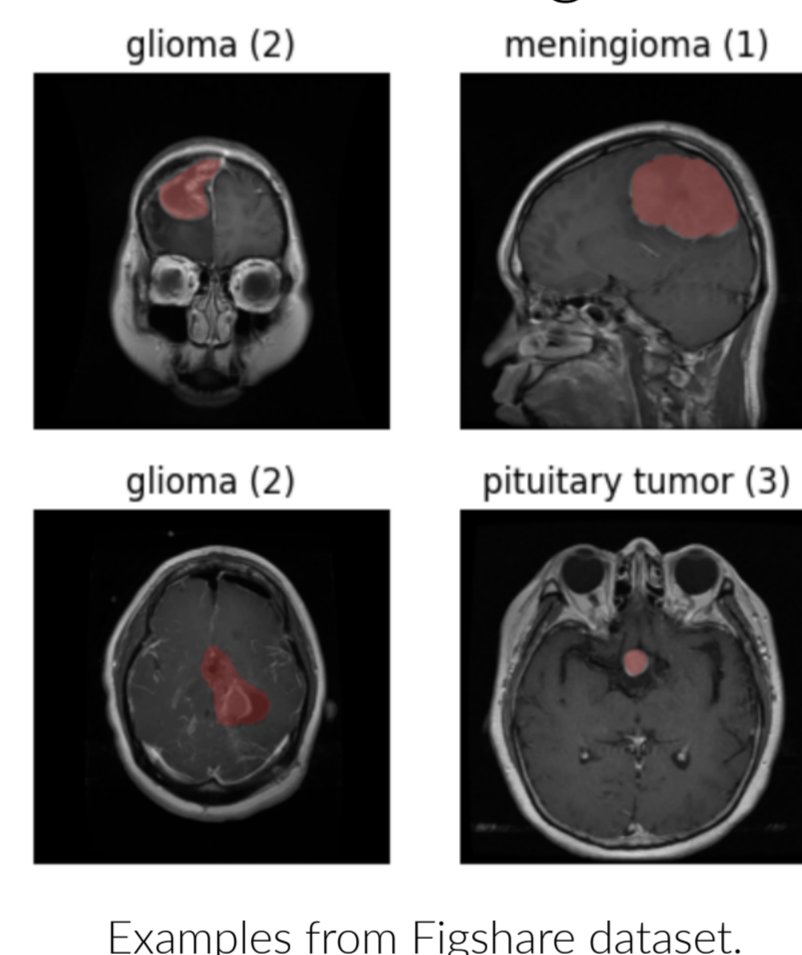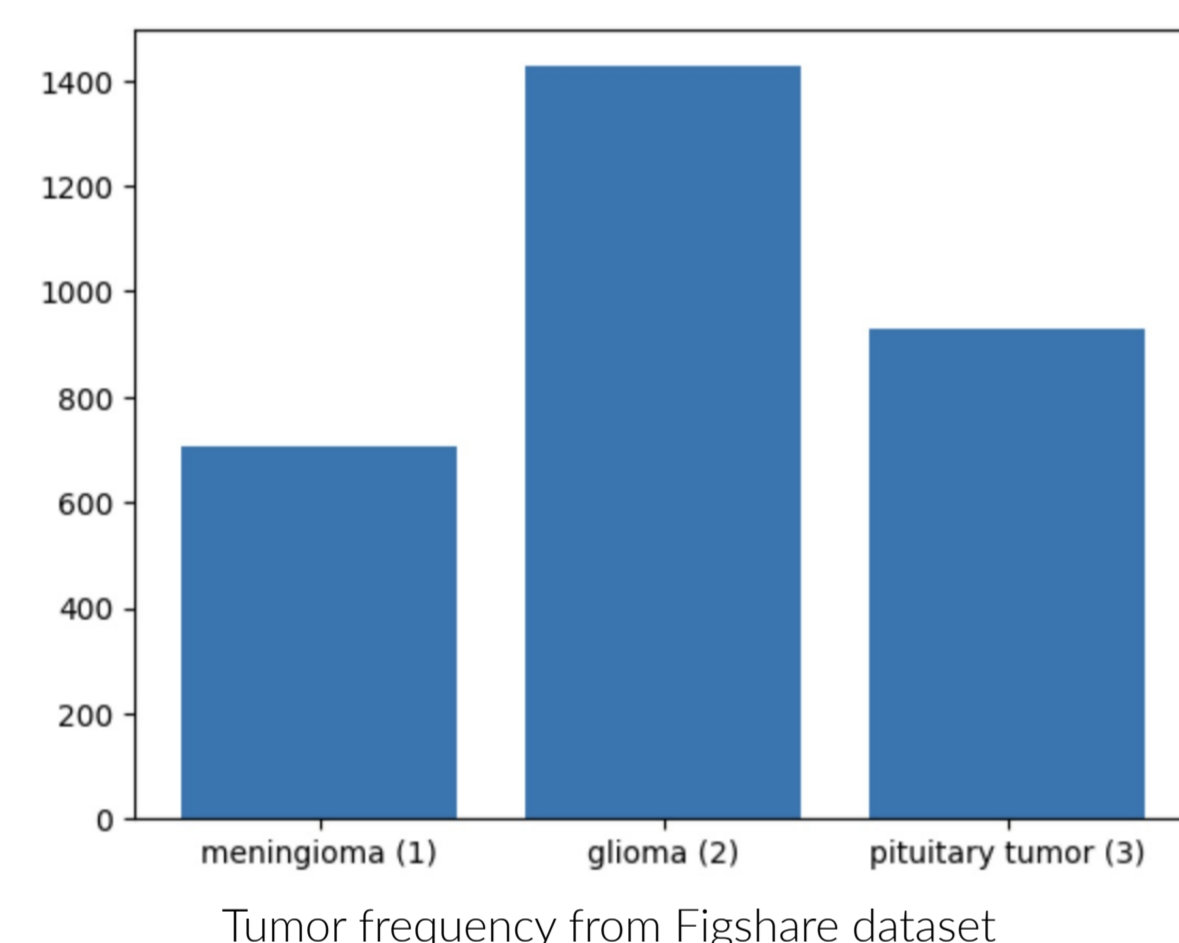
The dataset expanded from 3,064 to 9,192 images by applying rotations of 90° counter-clockwise and flipping each original image along the horizontal axis.

Model introduction & Architecture

Badža et al. [1] detailed one of the first attempts to specialize deep learning techniques to brain tumor classification. We replicated the architecture using Tensorflow and attained an accuracy of 93.4% with our chosen dataset. The model is organized into classification blocks, which gradually extract higher-level information from the MRI scan:

- **Convolutional Layer** - To share information between patches of the image.
- **ReLU activation** - To ensure the model can learn non-linear relationships between features.
- **Dropout Layer** - So that a single pixel or region of the image does not overly influence the classification decision.
- **Max-Pooling Layer** - To maintain invariance against small perturbations in the input which should not change the classification decision.

Finally, a fully connected layer learns the relationship between these features and tumor classes, followed by a softmax activation.
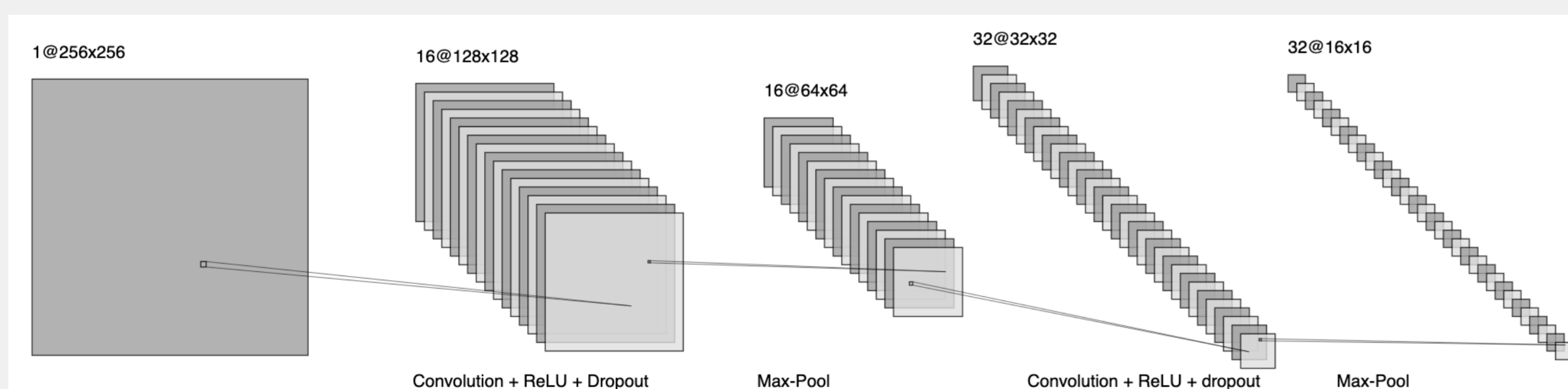

Figure 1. Model architecture composed of classification blocks

Model Training

We employed subject-wise cross-validation by dividing the dataset into 10 distinct folds, ensuring each patient appears in exactly one fold. Two folds are allocated for testing, two for validation, and the remaining six for training.
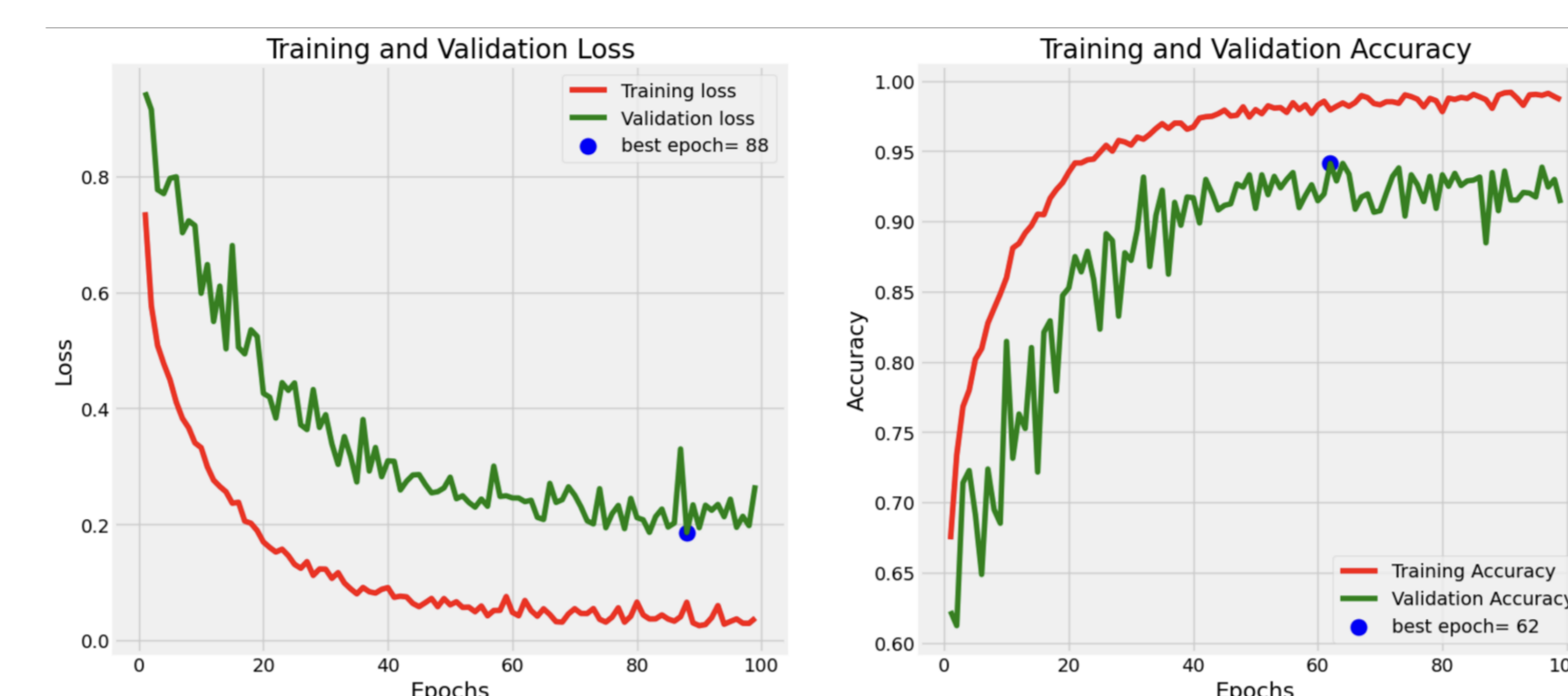

Figure 2. The figure displays training curves indicating the training and validation loss. Training was halted once the validation loss did not improve for consecutive 11 epochs, to prevent overfitting. Training and validation accuracies consistently increased at similar rates overall.

Division/Dataset	Testing Approach	Test Accuracy
Original Dataset	*One Test*	91.9%
Augmented Dataset	*One Test*	93.4%
Augmented Dataset	*Subject-Wise*	91.3%, $\sigma = 2.4\%$

Result of the model when trained on original and augmented datasets

## Model Interpretability: Saliency maps

Applying the vanilla gradient method, we derived the highest class probability across the entire image. The saliency map first concentrated on a small corner, and even after scaling, it still provided limited insight into the tumor's location.
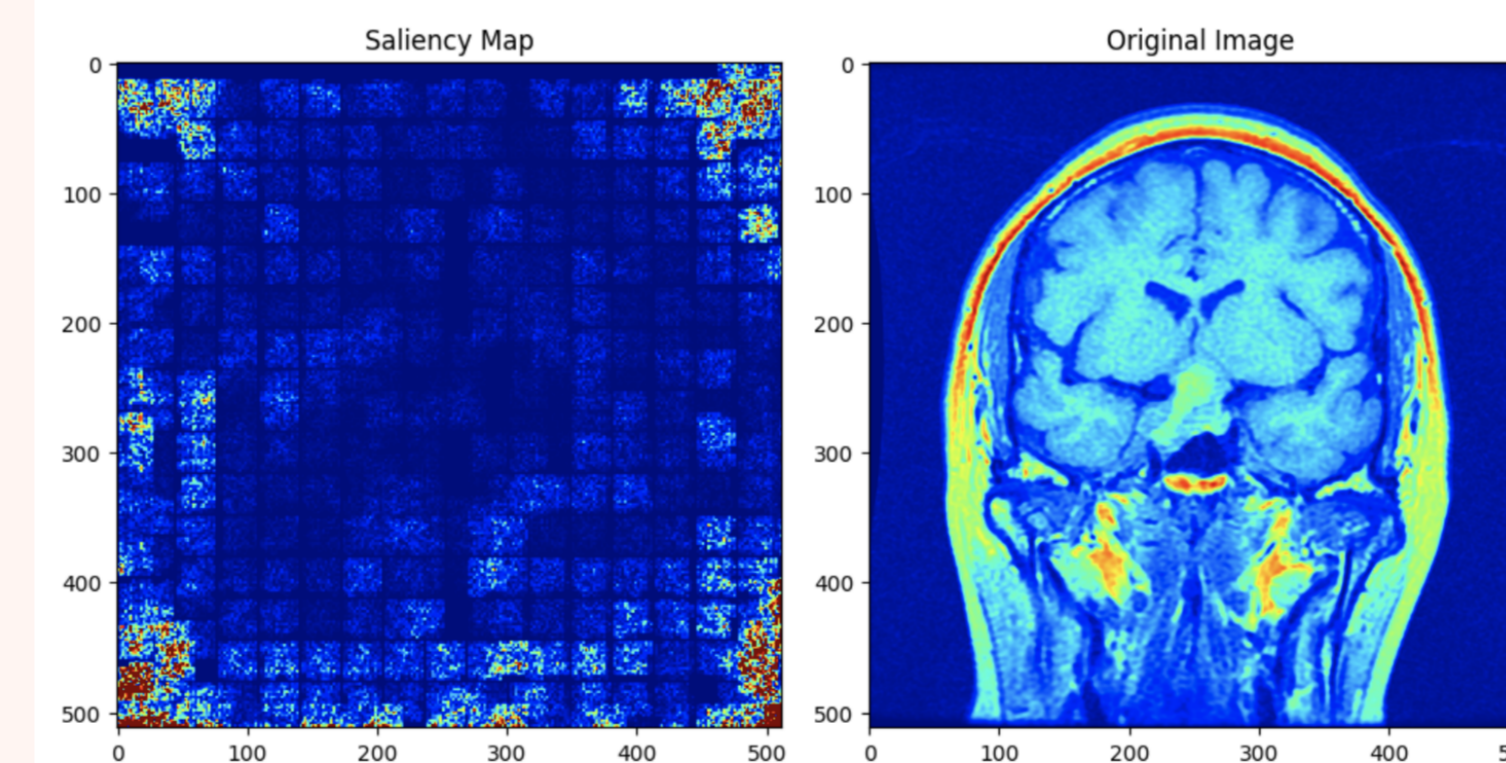
Our first saliency map implementation.

Observation: Vanishing Gradients

Per Brima et al [2], while the dataset and augmentation could contribute to this grid-like pattern in the saliency maps, the model architecture significantly influences this disparity. Model weights were primarily below one and predominantly zero gradients, even in areas where higher gradients were expected, which resulted in small gradients within the saliency map. A brief weight amplification retraining notably improved saliency map clarity.
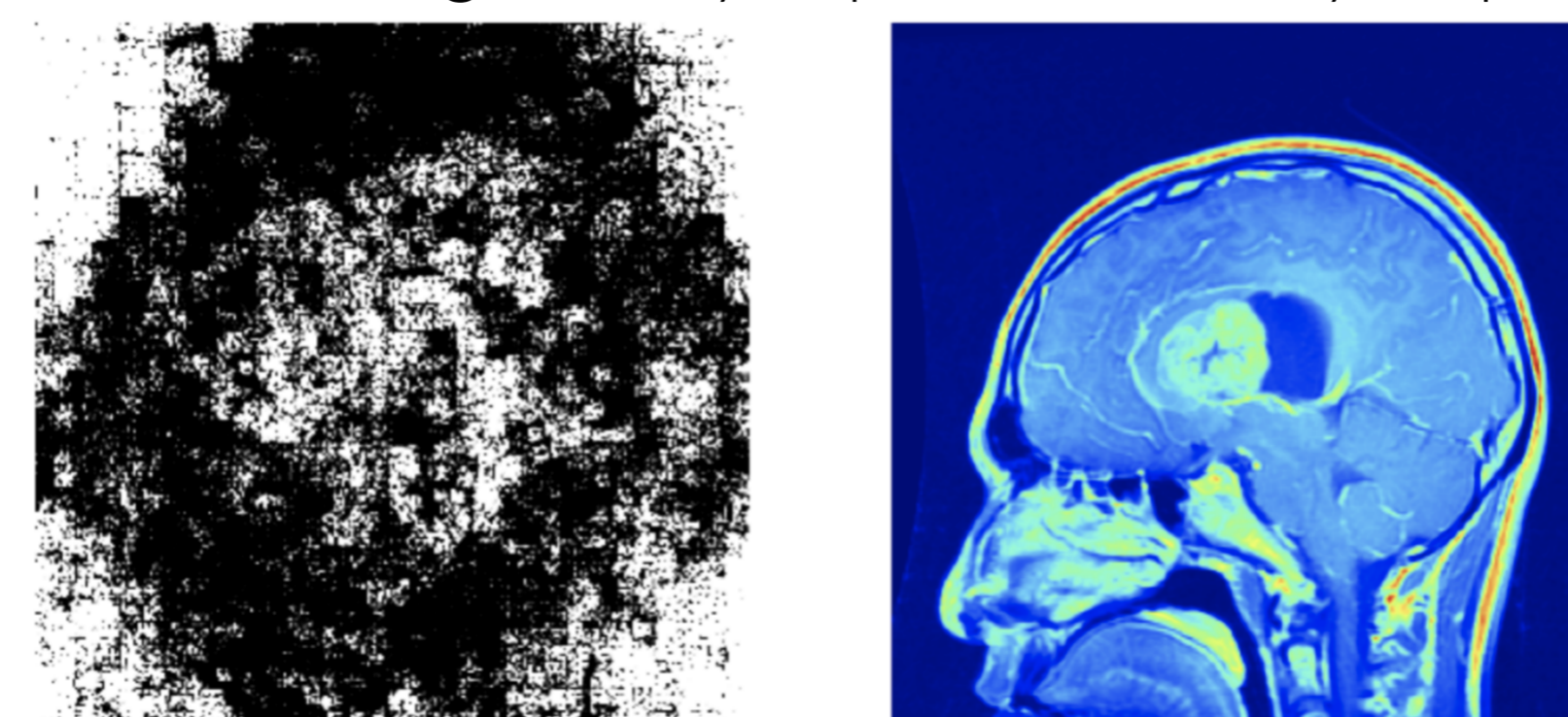
Improved saliency map

Adding Gaussian Noise

We experimented with adding Gaussian noise to enhance the saliency map, due to the consistent pixel values in the image background, as suggested by Professor Bonner. The assumption was that the model might have significant weights in the corners due to the near-zero pixel values, potentially overshadowing critical weights. However, this did not yield the expected result.
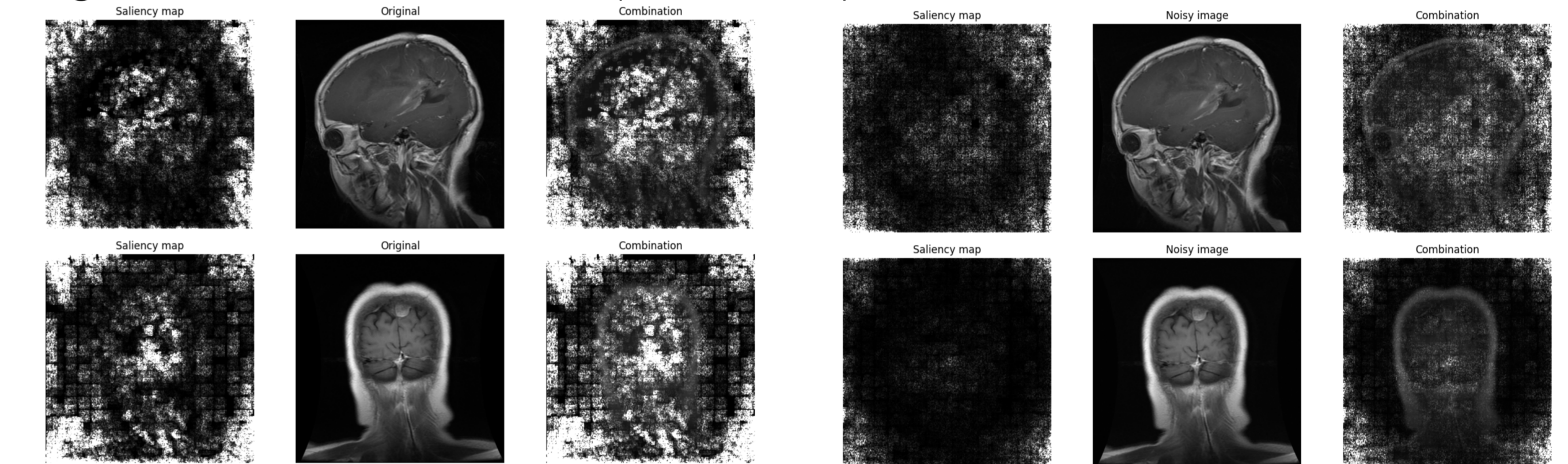
The improved Saliency map without noise

The improved Saliency map with noise

Model Robustness

Through data augmentation, generating new training examples by applying various transformations to the existing data, helped the model learn invariant features. While doing so, we ensured that augmented data generated from any given patient remained in the same fold as all the original data from said patient. This allowed the model to focus on features indicating tumour class that would remain the same given the listed transformations applied.

Conclusion

Seeking an efficient brain tumor classification model, our focus spanned refining detection methods and understanding decision-making. Subject-wise cross-validation prevented overfitting, enhancing adaptability across diverse patient data. Augmenting the dataset improved accuracy and fortified the model against input variations. Exploring interpretability methods revealed insights into the model's decisions. While facing challenges like vanishing gradients and Gaussian noise experiments, our model served as a learning platform, offering varied model development insights despite limitations.

References

[1] Milica M Badža and Marko Č Barjaktarović. Classification of brain tumors from mri images using a convolutional neural network. *Applied Sciences*, 10(6):1999, 2020.

[2] Yusuf Brima and Marcellin Atemkeng. Visual interpretable and explainable deep learning models for brain tumor mri and covid-19 chest x-ray images. 2023.

[3] Jun Cheng. Figshare brain tumor dataset.

[4] Y. M. Ayano E. S. Biratu, F. Schwenker and T. G. Debelee. A survey of brain tumor seg- mentation and classification algorithms, September 2021.

[5] Faith Davis Seth Climans Emily Walker, Jiaqi Liu and Yan Yuan. https://braintumourregistry.ca/, June 2022.